Supplementary Materials

Results

PGN gel zymography

To determine whether the protein bound to and/or degraded PGN, we performed a gel zymography assay. Under the non-reducing conditions of this assay, two bands of similar molecular masses were observed in both the western blot and zymogram (Fig. S1B). These data suggest that non-reducing conditions introduce microheterogeneity in the EsPGRP1 molecule resulting in a doublet rather than the singlet band observed in a conventional western blot. The results of the zymography experiments confirm that EsPGRP1 proteins extracted directly from *E. scolopes* are capable of binding to or breaking down PGN.

NanoSIMS

To assess the possibility that TCT could be directly interacting with EsPGRP1, we attempted to localize TCT within the light organ using nano secondary ion mass spectroscopy (NanoSIMS), a technique that maps the distributions of stable isotopes with a resolution comparable to electron microscopy (Lechene et al., 2006). ^{15}N-labeled TCT (^{15}N-TCT) was purified from *Bordetella pertussis* grown on ^{15}N-glutamate as the predominant carbon/nitrogen source. Incorporation of the stable isotope into TCT was verified by examination of the purified ^{15}N-TCT by NanoSIMS (data not shown). Hatchling *E. scolopes* were treated with 50 μM ^{15}N-TCT for durations spanning from 15 min to 24 h, and examined for deviations from terrestrial ratio of ^{14}N/^{15}N within tissues (Fig. S4). High-resolution images of the light organ epithelia were obtained by examining the distribution of ^{14}N within the samples, but the ^{14}N/^{15}N ratio was, within analytical errors, homogenous throughout the samples, i.e. there was no evidence that the ^{15}N-TCT molecules specifically localizaed in the light organ tissues. Due to the inconclusive nature of these data, we could not support nor exclude the hypothesis that nuclear loss of EsPGRP1 was the result of direct interactions with TCT. However, should this hypothesis be correct, we would expect nuclear loss of EsPGRP1 to be restricted to apoptotic cells induced by TCT, and it was not (see main text for details).

Experimental procedures

Analysis of protein activity

PGN zymograms were used to assay for PGN-binding and/or NAMLAA activity in total soluble protein extracts as previously described (Kohler et al., 2007) with some modifications. Protein extracts were subjected to non-reducing SDS-polyacrylamide gel electrophoresis (no β-mercaptoethanol added to the sample) containing 0.2% lyophilized *Micrococcus lysodeikticus* cells and the proteins were renatured over a 48 h period by frequent washing of the gel with 25 mM Tris (pH 7.5) with 1% Triton-X-100. The zymogram was stained with 1% Methylene Blue in 0.1% KOH for 5 min and subsequently destained in 0.1% KOH. Areas of digested PGN appeared as clear bands (dark) against a light blue background.

NanoSIMS

Hatchling *E. scolopes* were bathed in 50 μM ^{15}N-TCT from 15 min up to 24 h, then fixed (2% paraformaldehyde, 2% glutaraldehyde, 0.1 sodium cacodylate, 3% sodium chloride, 4.5% sucrose) for 12 h at 4°C. Fixative was washed 3 times for 30 m (0.1 sodium cacodylate, 3% sodium chloride, 4.5% sucrose) at 4°C, followed by secondary fixation in 1% osmium tetraoxide in wash buffer for 1 h. Samples were rinsed 3 times in wash buffer buffer to remove any traces of secondary fixative, then dehydrated in an ethanol series. Specimens were transferred 2 times in 100% propylene oxide and then a 1:1 propylene oxide:epon mix (Electron Microscopy Sciences, Hatfield, PA) . Samples were cycled through 5 changes of unaccelerated 24 h, followed by 3 changes of accelerated epon and then polymerized at 60°C for 48 h. 0.5 μm thick sections were suspended on a drop of deionized H_20 and dried on 5x5 mm silicon chips (SPI supplies, West Chester PA). Sections were placed in a vacuum chamber, degassed and analyzed with a NanoSIMS 50 (Cameca, Nampa, ID). The NanoSIMS isotope imaging measurements were performed by rastering a Cs^+ primary beam over the sample and simultaneously collecting secondary ions of $^{12}C^-$, $^{13}C^-$, $^{12}C^{14}N^-$, and $^{12}C^{15}N^-$ as well as secondary electrons. Isotopic ratios of $^{14}N/^{15}N$ were obtained by dividing the images of $^{12}C^{14}N$ and $^{12}C^{15}N$.

Plasmid construction

The *ltgA* and *ltgD* genes were cloned into shuttle vector pVSV107 (Dunn et al., 2006) to generate plasmids pDMA196 and pDMA190, respectively. The construction of pDMA196 has been described elsewhere (Adin *et al.*, 2008). pDMA190 was generated by first PCR amplifying *ltgD* with primers dma103 (5' GGG TGA AAT TAC TGC CCT TTA AAT CG 3') and dma104 (5' GCG CCC GGG GGA TCC TTA CTT AAT CGA ATC AGC CAA GTG ACT TAC 3'), cloning the *ltgD*-containing fragment into pCR-BluntIITOPO (Invitrogen, Carlsbad, CA) to generate pDMA178, and then subcloning the *ltgD*-containing *Kpn*I-*Xba*I fragment from pDMA178 into *Kpn*I- and *Xba*I-digested pVSV107. The PCR product cloned in pDMA178 was sequenced to ensure that no unintended base pair changes were generated in the amplification process.

References

Adin, D.M., Engle, J.T., Goldman, W.E., McFall-Ngai, M.J. and Stabb, E.V. (2008). Mutations in ampG and lytic transglycosylase genes affect the net release of peptidoglycan monomers from *Vibrio fischeri*. *J Bacteriol*.

Dunn, A.K., Millikan, D.S., Adin, D.M., Bose, J.L. and Stabb, E.V. (2006). New rfp- and pES213-derived tools for analyzing symbiotic *Vibrio fischeri* reveal patterns of infection and *lux* expression in situ. *Appl Environ Microbiol* **72,** 802-810.

Kohler, P.L., Hamilton, H.L., Cloud-Hansen, K. and Dillard, J.P. (2007). AtlA functions as a peptidoglycan lytic transglycosylase in the *Neisseria gonorrhoeae* type IV secretion system. *J. Bacteriol.* **189,** 5421-5428.

Lechene, C., Hillion, F., McMahon, G., Benson, D., Kleinfeld, A.M., Kampf, J.P*., et al.* (2006). High-resolution quantitative imaging of mammalian and bacterial cells using stable isotope mass spectrometry. *J Biol* **5,** 20.

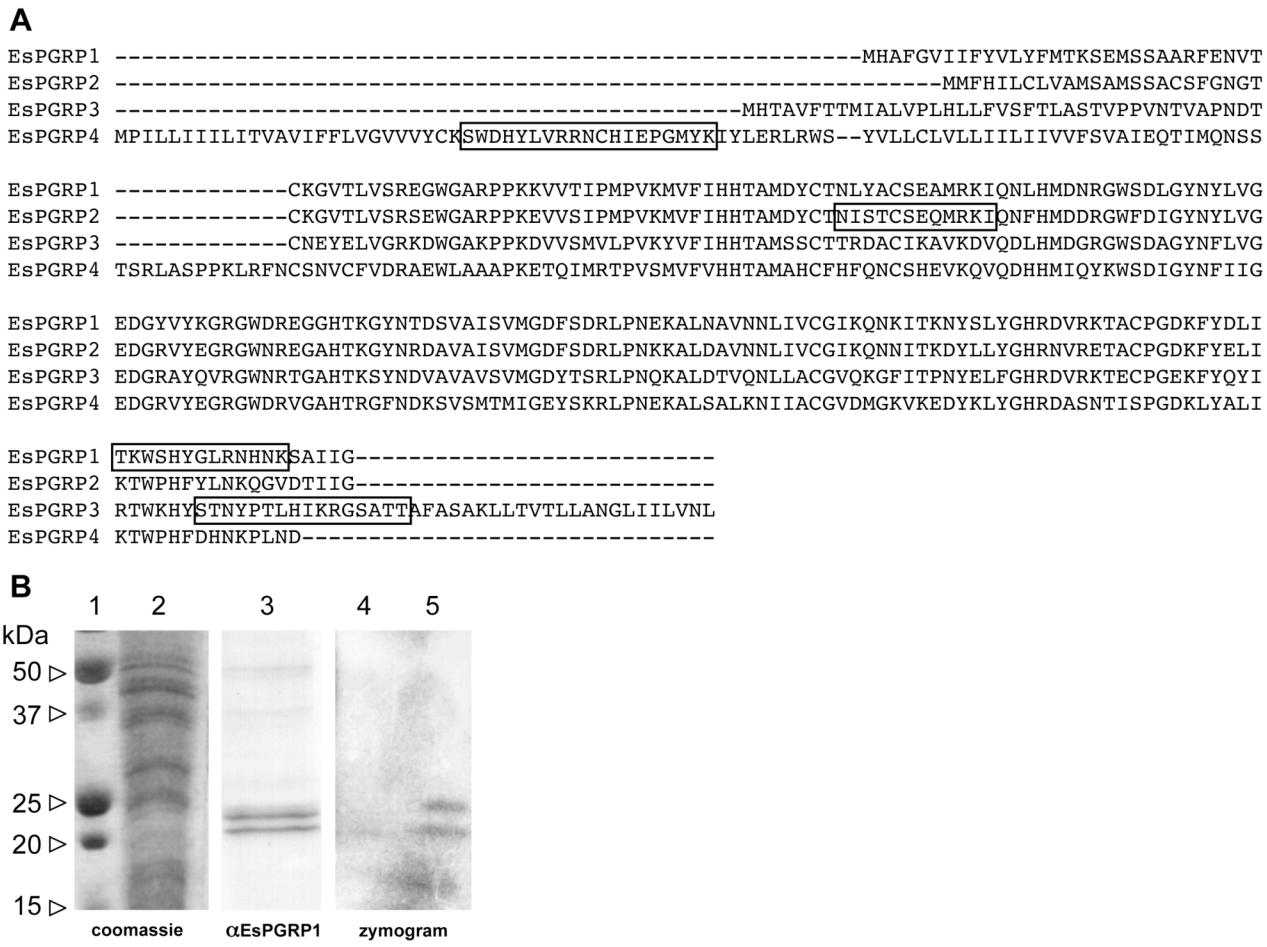

Figure S1. Antibody generation and PGN-gel zymography

A) Clustal W alignment of all four EsPGRPs. Boxed areas indicate sequences used for synthetic peptide antigens to raise specific anti-EsPGRP antibodies. B) A representive non-reducing zymogram of *E. scolopes* protein extracts and accompanying immunoblot. Non-reducing SDS-PAGE gels of the aqueous protein fraction show correspondance between proteins that react with anti-EsPGRP1 antibody and those that degrade PGN (dark bands on zymogram). 1, MW standards; 2, coomassie stained tissue extract; 3, anti-EsPGRP1 immunoblot; 4, empty zymogram lane; 5, zymogram of aqueous protein fraction.

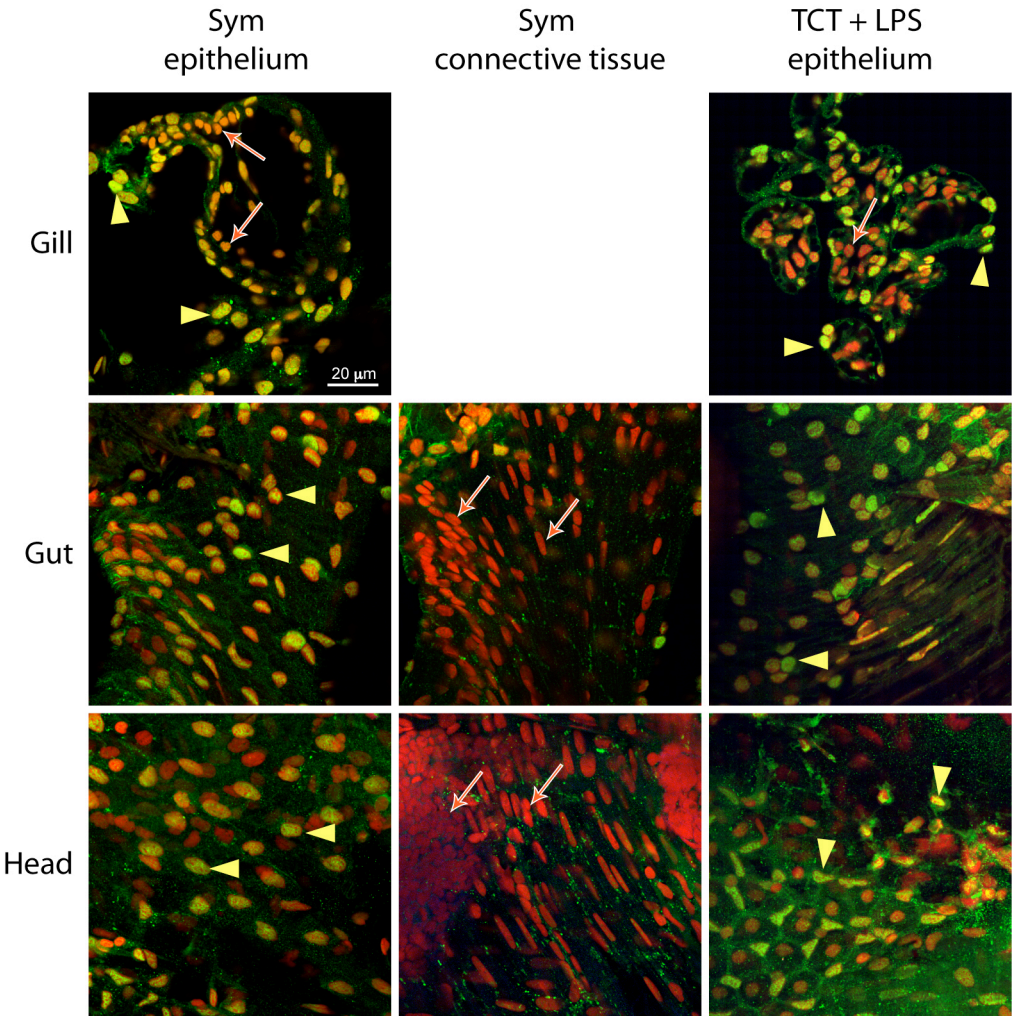

Figure S2. Localization of EsPGRP1 in symbiotic or TCT-treated *E. scolopes* epithelia

Representative confocal micrographs of gill, gut and head tissues from animals colonized by *V. fischeri* or treated with 10 μM TCT + 10 ng/ml LPS. Epithelial nuclei contained EsPGRP1 (yellow arrowheads) whereas non-epithelial nuclei from the gut or head connective tissues or hemocytes in the gills did not stain for EsPGRP1 (red arrows). EsPGRP1, green; DNA, red; TUNEL, blue.

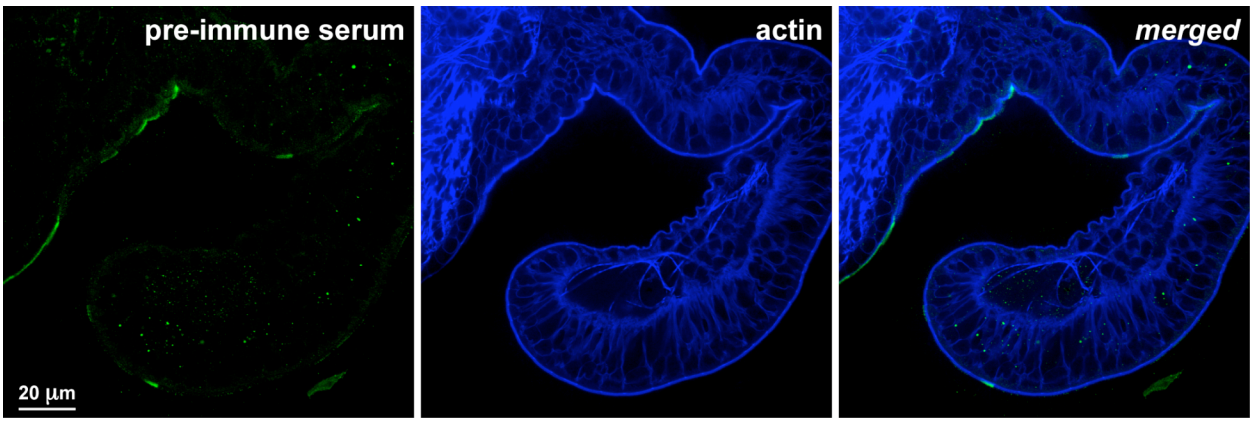

Figure S3. Nonreactivity of pre-immune serum with *E. scolopes* tissues

Representative confocal micrographs of the *E. scolopes* light organ exposed to a 1:100 dilution of serum obtained prior to exposure to the EsPGRP1 antigen. No significant cross reactivity was observed. Pre-immune serum, green; actin cytoskeleton, blue.

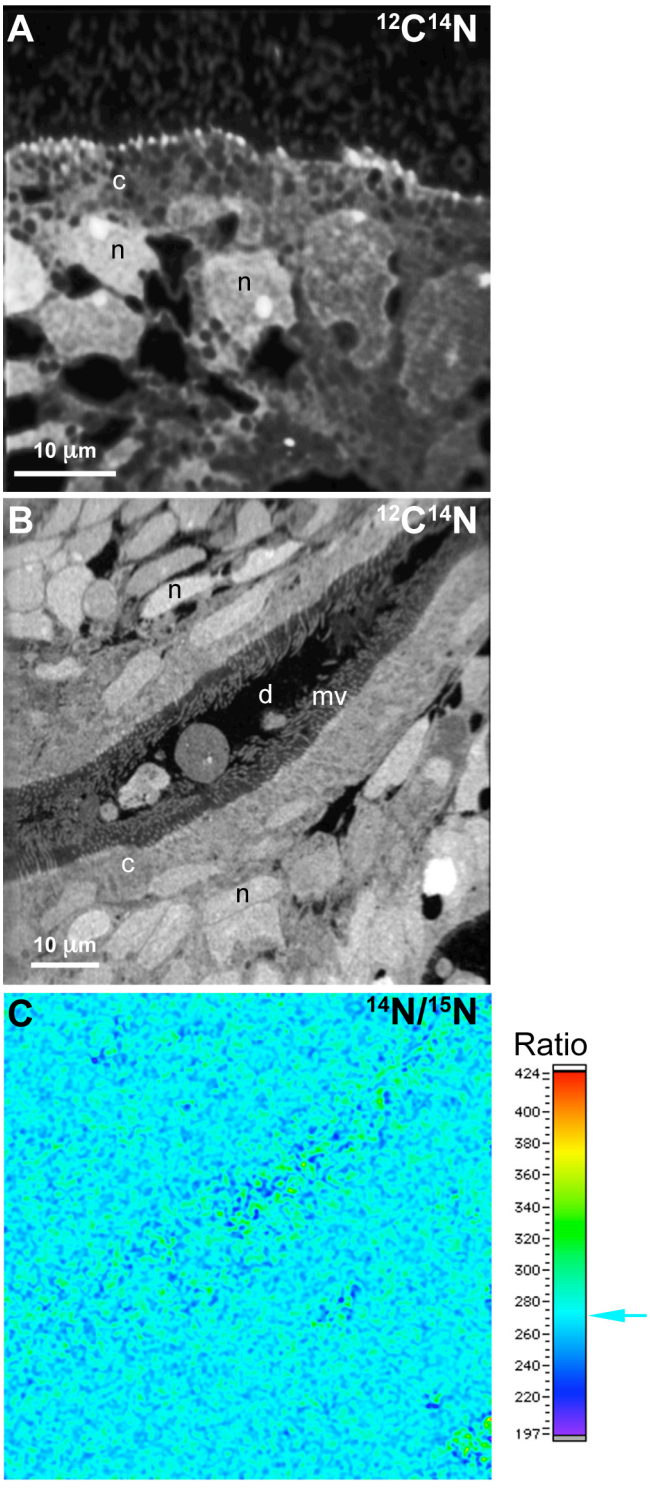

Figure S4. NanoSIMS tracing of ^{15}N-TCT in light organ sections

Representative NanoSIMS images of $^{12}C^{14}N$ distribution in A) the anterior appendage or B) the duct. C) Representative NanoSIMS image of the distribution of $^{12}C^{14}N$ divided by the distribution of $^{12}C^{15}N$ in the area shown in B. The standard terrestrial ratio of $^{12}C^{14}N$ to $^{12}C^{15}N$ is ~270 (color indicated by arrow on color scale). No observed deviations from this value were statistically significant. Apparent patterns, such as that in the duct lumen, reflect increased variation due to low signal. c, cytoplasm; d, duct lumen; mv, microvilli; n, nucleus.